



## Characterization of cubic phase MgZnO/Si(1 0 0) interfaces

J. Liang<sup>a</sup>, H.Z. Wu<sup>a,\*</sup>, Y.F. Lao<sup>a</sup>, N.B. Chen<sup>b</sup>, P. Yu<sup>b</sup>, T.N. Xu<sup>b</sup>

<sup>a</sup> State Key Laboratory of Functional Materials for Informatics,  
Shanghai Institute of Microsystem and Information Technology,  
Chinese Academy of Sciences, 865 Changning Road, Shanghai 200050, China  
<sup>b</sup> Department of Physics, Zhejiang University, Hangzhou 310027, China

Received 19 January 2005; received in revised form 2 February 2005; accepted 2 February 2005  
Available online 17 March 2005

### Abstract

The microstructural properties of the Mg<sub>x</sub>Zn<sub>1-x</sub>O/Si(1 0 0) interface were investigated using transmission electron microscopy (TEM) and chemical states of the heterostructure were studied by high resolution X-ray photoelectron spectroscopy (XPS). By analyzing the valence band spectra of thin Mg<sub>x</sub>Zn<sub>1-x</sub>O/Si(1 0 0) heterostructures, the valence band offset between such Mg<sub>0.55</sub>Zn<sub>0.45</sub>O and Si(1 0 0) was obtained to be 2.3 eV. Using the cubic ternary thin films as insulators, metal–insulator–semiconductor (MIS) capacitors have been fabricated. Leakage current density lower than  $3 \times 10^{-7}$  A/cm<sup>2</sup> is obtained under the electrical field of 600 kV/cm by current–voltage (*I*–*V*) measurement. Frenkel–Poole conduction mechanism is the main cause of current leakage under high electrical field.

© 2005 Elsevier B.V. All rights reserved.

**Keywords:** MgZnO thin film; Band offset; MIS structure; Leakage mechanism

### 1. Introduction

The continued scaling down of complementary metal-oxide semiconductor (CMOS) technology is pushing the thickness of SiO<sub>2</sub> towards 1 nm as the gate dielectric. Owing to its unacceptable tunneling leakage current and intrinsic reliability concerns, SiO<sub>2</sub> is reaching its physical limit. Alternative gate dielectrics are very desirable to meet the technological

requirement of CMOS. Utilizing an insulator with a higher dielectric constant than that of SiO<sub>2</sub> (i.e., a high-*k* dielectric) enables the use of a larger physical thickness to maintain the same capacitance. In the recent years, there has been much interest in the zinc oxide (ZnO) materials and fabrication of ZnO-related heterostructures. Novel cubic Mg<sub>x</sub>Zn<sub>1-x</sub>O ( $x \geq 0.50$ ) epitaxial heterostructures on Si(1 0 0) substrates were synthesized by pulsed laser deposition (PLD) [1] and reactive electron beam evaporation deposition (REBED) at low growth temperature [2]. Optical properties including wide band gap ( $E_g > 5.0$  eV) were reported previously [3]. The temperature-

\* Corresponding author. Tel.: +86 21 625 11070;  
fax: +86 21 625 13510.  
E-mail address: [hzwu@mail.sim.ac.cn](mailto:hzwu@mail.sim.ac.cn) (H.Z. Wu).

dependent bandgaps of the cubic phase  $\text{Mg}_x\text{Zn}_{1-x}\text{O}$  films have been measured by ultraviolet optical transmission with temperature variation from 10 to 300 K and analyzed by theoretical simulating the optical absorption spectra [4]. Indices of refraction for cubic phase  $\text{Mg}_x\text{Zn}_{1-x}\text{O}$  ( $0.57 \leq x \leq 1$ ) thin film alloys were obtained to be between 1.89 and 1.70 by transmission spectra and Manifacier method [5]. The electrical properties including high dielectric constant ( $\epsilon \sim 10.5$ ) and low leakage current were attended [3]. These properties of the new material are rendering new applications such as application in micro- and nano-electronic devices [6,7].

As a candidate of high- $k$  material for dielectric oxides, the interface in direct contact with channel region in MOS must be engineered to permit low interface trap density (e.g. dangling bonds) and minimize carrier scattering (maximize mobility in the channel) in order to obtain reliable and high performance. Another crucial requirement for high- $k$  material is low leakage currents. It is desirable to find a gate dielectric that has large  $\Delta E_c$  value to Si, the conduction band offset, and perhaps to other gate metals which may be used. If the experimental  $\Delta E_c$  values for these oxides are even much less than 1.0 eV, it will likely preclude the applications of these oxides as gate dielectrics because electron transport (either by thermal emission or tunneling) would lead to unacceptably high leakage currents [8]. The values  $\Delta E_c \sim 2.3$ – $2.8$  eV for  $\text{Al}_2\text{O}_3$  and  $\text{Y}_2\text{O}_3$ , and  $\Delta E_c \sim 1.5$  eV for  $\text{ZrO}_2$  and  $\text{ZrSiO}_4$  were reported by Roberson [9].

In this report, we use X-ray photoelectron spectroscopy (XPS) to demonstrate the conduction band offset  $\Delta E_c$  of cubic phase  $\text{MgZnO}$  epitaxial layer to Si. Using the cubic ternary thin films as insulators, metal–insulator–semiconductor (MIS) capacitor structures have been fabricated. Current–voltage ( $I$ – $V$ ) characteristics were analyzed to explore the leakage mechanism in the film under high electrical field.

## 2. Experiment

Cubic phase  $\text{Mg}_x\text{Zn}_{1-x}\text{O}$  ( $x > 0.5$ ) layers were deposited by a reactive e-beam evaporation system on  $p$ -type Si(100) wafers with a resistivity of 1–5  $\Omega$  cm. Since Si wafers usually have an ultra thin native  $\text{SiO}_x$

layer of 1–5 nm on top of the Si substrate, a 0.5% HF strip of the surface chemical oxide was followed by pure water rinse to eliminate residual Si–F bonds prior to the deposition of  $\text{Mg}_x\text{Zn}_{1-x}\text{O}$  dielectric layer. The  $\text{Mg}_x\text{Zn}_{1-x}\text{O}$  layers were deposited at 250 °C in oxidation ambient with chamber pressure of  $2 \times 10^{-4}$  Torr. The details of growth of cubic phase  $\text{Mg}_x\text{Zn}_{1-x}\text{O}$  thin film and the determination of Mg composition were published in the references [3,5]. The thicknesses of the  $\text{Mg}_x\text{Zn}_{1-x}\text{O}$  dielectric layers varied between 80 and 300 nm measured by Taylor-Hobson Talystep.

To characterize chemical and electronic structure of the films, high-resolution XPS was carried out utilizing monochromatized Al  $K\alpha$  (1486.6 eV) radiation by Perkin-Elmer PHI 5000C ESCA System. The core levels such as  $\text{Si}_{2p}$ ,  $\text{Mg}_{2p}$  and  $\text{Zn}_{2p}$ , and the valence band spectra of the samples were taken at photoelectron take-off angles of 45° and 90°. To fabricate MOS capacitors, 300 nm Al layer was deposited on  $\text{Mg}_x\text{Zn}_{1-x}\text{O}$  and then 450 °C rapid thermal processing (RTP) treatment for Ohm contact was preceded. MOS capacitors were defined on the gate dielectric stacks by lithography through a shadow mask with a capacitor area of 0.15 mm<sup>2</sup>. The oxide leakage current characteristics were measured using HP 4156 Precision Semiconductor Parameter Analyzer.

## 3. Results and discussion

### 3.1. Micro-structural features at interface of $\text{MgZnO/Si}(1\ 0\ 0)$

Fig. 1 (a) shows cross-section TEM micrograph from a sample of  $\text{Mg}_{0.55}\text{Zn}_{0.45}\text{O}$  thin film deposited on Si(1 0 0) substrate. The cross-section micrograph clearly shows the interface between the Si substrate and  $\text{Mg}_{0.55}\text{Zn}_{0.45}\text{O}$  epitaxial layer, which exhibits a polycrystalline structure. The magnified grain configuration is shown in the inset. We note that the size of crystal grains is about tens nanometer. Similar images are observed along the interface between the epitaxial layer and Si substrate. In Fig. 1(b), we show micro-diffraction patterns from the epitaxial layer. From these diffraction studies, it is clearly evident that the synthesized  $\text{Mg}_{0.55}\text{Zn}_{0.45}\text{O}$  films possess cubic symmetry with cube-on-cube alignment. This is consistent

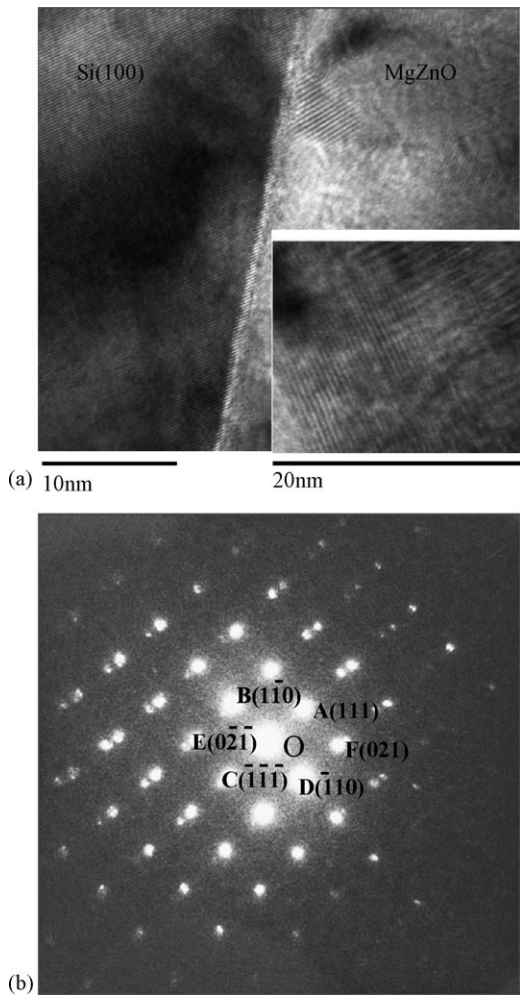


Fig. 1. (a) FE-TEM images of cubic  $Mg_{0.55}Zn_{0.45}O$  by REES methods and inset is the detail of cubic crystal grain region. (b) The micro-diffraction patterns of the cubic  $Mg_{0.55}Zn_{0.45}O$  film.

with X-ray diffraction of high (1 0 0) orientation. The couple highlight points represent the overlap crystal grain.

To investigate the characteristics of interface between the oxide and silicon substrate, XPS characterization was performed. Fig. 2(a) shows Si 2p spectra taken from the sample with 2 nm thick  $Mg_{0.55}Zn_{0.45}O$  on Si(1 0 0). The measured Si 2p spectrum can be represented by summing the spectra of various oxidation states. To investigate the oxidation states more quantitatively, we fitted the spectra using a standard curve-fitting procedure

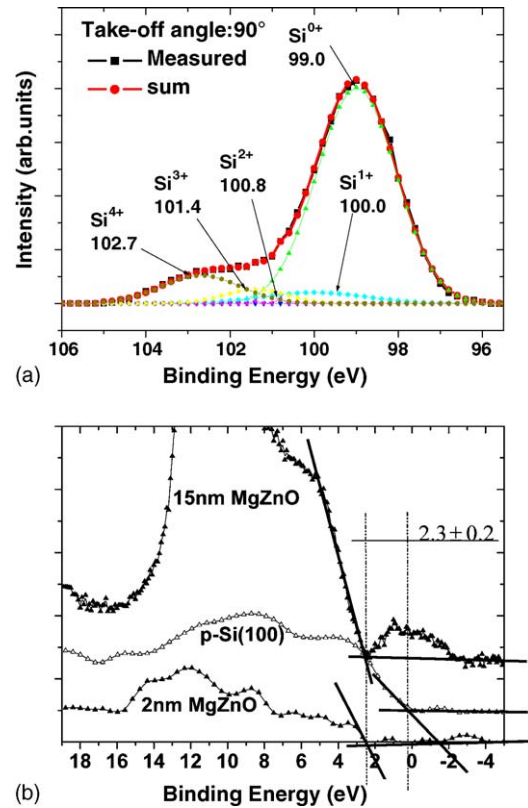


Fig. 2. (a) Si 2p XPS spectrum is measured at the take-off angle of  $90^\circ$  (fine solid line) and the components of Si substrate ( $Si^{0+}$ ) and suboxides ( $Si^{1+}$ – $Si^{4+}$ ) are denoted; (b) O 1s XPS spectrum.

provided by the XPS manufacturer. The fully oxidized states of Si atoms shown in the Fig. 2(a) are  $Si^{4+}$  in the  $SiO_2$  thin film, bulk states in the substrate are  $Si^{0+}$ , and intermediate oxidation states  $Si^{1+}$ ,  $Si^{2+}$ ,  $Si^{3+}$  in the transition layer [10]. It is seen that the states of  $Si^{0+}$  dominate the spectrum and the density of intermediate oxidation states ( $Si^{1+}$ ,  $Si^{2+}$ ,  $Si^{3+}$ ) is small. From Fig. 2, it is seen that the energy shift of  $Si^{4+}$  component from the substrate component ( $Si^{0+}$ ) is 3.7 eV, which has a good fit to the measured spectrum. It indicates that silicon dioxide with Si binding energy of 102.7 eV are almost completely formed at the interface. The density of  $Si^{2+}$  component with chemical shift from  $Si^{0+}$ , being 1.8 eV, is smallest. The XPS signal intensity ratio of bulk silicon and the oxide components are  $Si^{0+}:Si^{1+}:Si^{2+}:Si^{3+}:Si^{4+} = 573:35:1:30:73$ .

As shown in the Fig. 2(b), the O 1s XPS spectrum shows a single peak at 531 eV. Signal of Si–O bond at 532 eV is not observed. However, Miyazaki observed

strong Si–O signal of 532 eV at the interface of ZrO<sub>2</sub>/Si(1 0 0) with the formation of interfacial oxide layer as thin as 1.7 nm, by 500 °C annealing in dry O<sub>2</sub> for 5 min [11]. Therefore, it can be concluded that the silicon oxides at the interface is in monolayer scale because the Mg<sub>0.55</sub>Zn<sub>0.45</sub>O layer on Si was grown at low temperature. Fig. 3(a and b) shows Mg 2p and Zn 2p spectra. The Mg 2p shifts positive 0.6 eV from the Mg 2p (MgO) with binding energy of 50.80 eV, while the Zn 2p shifts negative 0.6 eV from the Zn 2p (ZnO) with binding energy of 1021.75 eV. The shift of binding energy could be related to the formation of ternary MgZnO alloy film.

For thin gate dielectrics, the interface with Si plays a key role and in most cases is a dominant factor in determining the overall electrical properties. Thermodynamic stability of the MgZnO/Si(1 0 0) interface is an important issue. A comprehensive investigation of the thermodynamic stability of binary oxides in

contact with silicon was conducted by Schlom et al. [12]. It was concluded that MgO is thermodynamically stable in contact with silicon at 1000 K, while Zn–O bonds are not stable in contact with Si at such a high temperature [13]. Our previous Auger electron spectrometry (AES) depth profiles for the as-grown MgZnO films (with growth temperature of 250 °C) demonstrated good uniformity of Mg, Zn and O components over 60 nm film thickness [14]. However, after high temperature (900 °C) annealing under O<sub>2</sub> ambient, distinct profile change of Zn concentration in the film and at interfacial region was observed. The changes of Zn profile indicate the breaking of Zn–O bonds in contact with Si and Zn migrating towards the surface at such high annealing temperature. In contrast, Mg component profile was still uniformly distributed after the MgZnO films were annealed at 900 °C under O<sub>2</sub> ambient, indicating MgO is stable at such a high annealing temperature [14]. These AES observations are consistent with Schlom's results.

### 3.2. Analysis of valence band spectra and determination of energy band alignments

To obtain the valence band offset of Mg<sub>0.55</sub>Zn<sub>0.45</sub>O/Si heterostructure, valence band spectra was measured by low energy XPS. Two Mg<sub>0.55</sub>Zn<sub>0.45</sub>O/Si heterostructure samples were prepared with Mg<sub>0.55</sub>Zn<sub>0.45</sub>O film thicknesses of 2 and 15 nm. Fig. 4(a) shows the valence band spectrum for Mg<sub>0.55</sub>Zn<sub>0.45</sub>O (2 nm)/Si(1 0 0) heterostructure and reference spectrum measured from Si(1 0 0) substrate. Then the spectrum for Mg<sub>0.55</sub>Zn<sub>0.45</sub>O film was obtained by subtracting the reference spectrum of Si(1 0 0) substrate from the measured spectrum for Mg<sub>0.55</sub>Zn<sub>0.45</sub>O/Si(1 0 0) heterostructure. Fig. 4(b) shows the valence band photoelectron energy-distribution curves for the two Mg<sub>0.55</sub>Zn<sub>0.45</sub>O coverages (2 and 15 nm) and for Si(1 0 0) substrate. The binding energy of each valence band spectrum was calibrated by the energy position of the corresponding C 1s peak of the surface and Si 2p of the Si(1 0 0) substrate. For 15 nm thick Mg<sub>0.55</sub>Zn<sub>0.45</sub>O film in which XPS signal from Si(1 0 0) substrate could not be detected, the binding energy of Zn 3d peak (10.7 eV) in Fig. 4(b) was referred to see the valence band edge of Mg<sub>0.55</sub>Zn<sub>0.45</sub>O. Notice that the leading edges of valence-band for the two samples are clearly seen. A

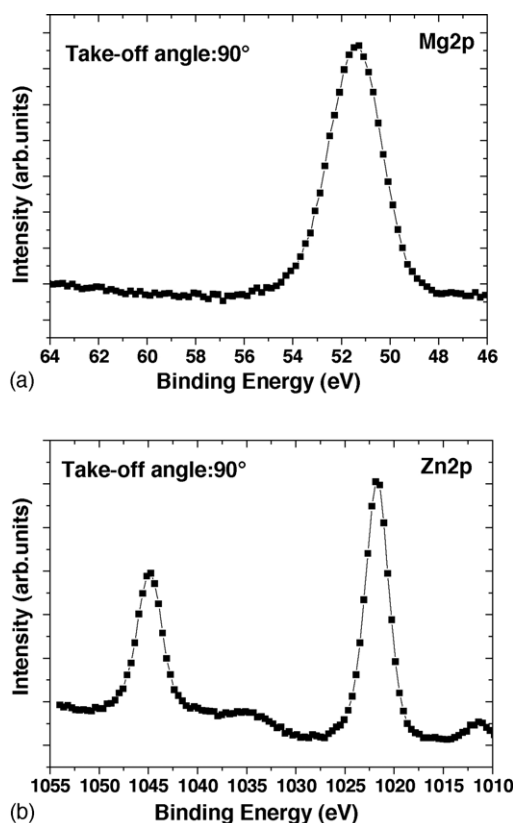


Fig. 3. XPS spectra of 2 nm thick Mg<sub>0.55</sub>Zn<sub>0.45</sub>O/Si(1 0 0): (a) Mg 2p; (b) Zn 2p.

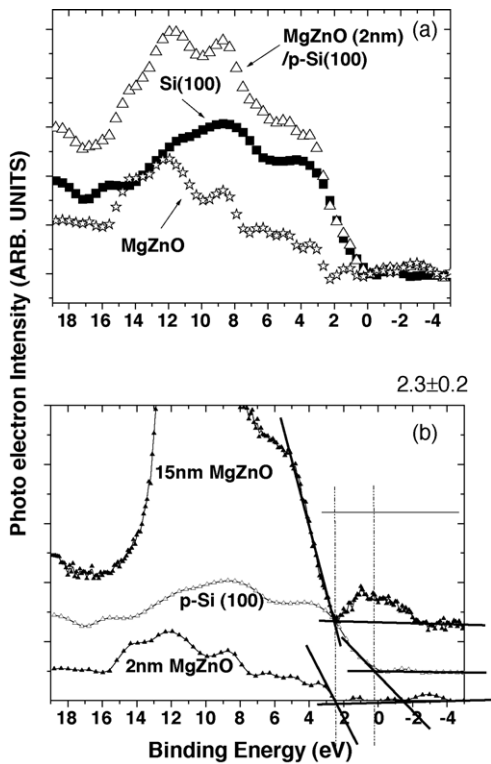


Fig. 4. (a) The measured valence band spectrum for  $Mg_{0.55}Zn_{0.45}O$  (2 nm)/Si(100) heterostructure and reference spectrum measured from Si(100) substrate; (b) the detail diagrammatic curve for the valence band offset  $\Delta E_v$  of the cubic  $Mg_{0.55}Zn_{0.45}O/Si(100)$  heterostructure.

direct measurement of valence band offset ( $\Delta E_v$ ) of  $Mg_{0.55}Zn_{0.45}O/Si$  heterostructure is possible in this case by linear extrapolation of the two edges [9]. The edge positions deduced by linear extrapolation were cross-checked for different systems with those deduced from the energy positions of the corresponding core levels. As a result, the valence band offset  $\Delta E_v$  at the interface of  $Mg_{0.55}Zn_{0.45}O/Si$  heterostructure is 2.30 eV. Considering the band gap energies of  $Mg_{0.55}Zn_{0.45}O$  (5.76 eV) [3] and Si (1.12 eV), as shown in the Fig. 5, the conduction band offset  $\Delta E_c$  is obtained to be 2.34 eV.

### 3.3. Leakage current and conduction mechanism

The Al/ $Mg_{0.55}Zn_{0.45}O$  (80 nm)/p-Si/Al MIS structures were fabricated with 0.15 mm<sup>2</sup> area of Al electrode on both of  $Mg_{0.55}Zn_{0.45}O$  surface and silicon

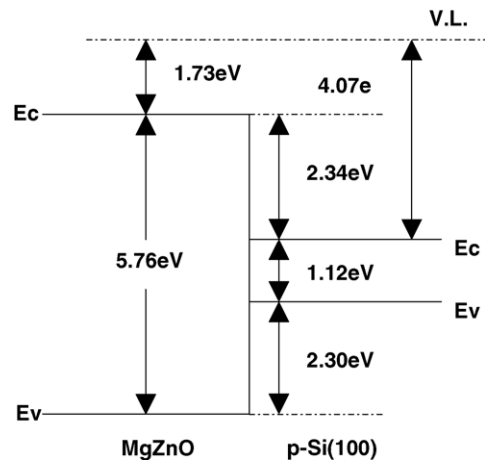


Fig. 5. Energy band profile for cubic  $Mg_{0.55}Zn_{0.45}O/Si(100)$  heterostructure.

substrate. Then it was annealed at 450 °C in N<sub>2</sub> atmosphere. The corresponding current–voltage (*I*–*V*) characteristic for the MIS structure is shown in Fig. 6. The leakage current density is as low as  $3 \times 10^{-7}$  A/cm<sup>2</sup> at the bias of 5 V (electrical field of  $\sim 600$  kV/cm). In contrast, similar MIS structure which is made of 65 nm thick SiO<sub>2</sub> layer as insulator has leakage current of approximately  $4 \times 10^{-4}$  A/cm<sup>2</sup>, nearly three orders of magnitude higher than that of the  $Mg_{0.55}Zn_{0.45}O$  insulator devices. The measured leakage current at room temperature consists of three different conduction mechanisms including Ohm current, Fowler-Nordheim (F-N) tunneling current

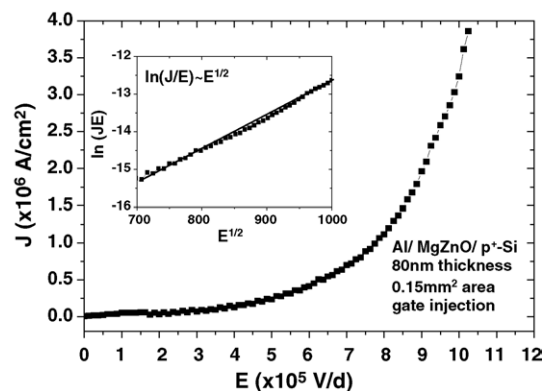


Fig. 6. Leakage current density vs. electrical field for the Al/ $Mg_{0.55}Zn_{0.45}O/Si(100)/Al$  MIS structure. The inset is the fitting results of F-P conduction.

and Frenkel-Poole (F-P) current which is generated from the defects and electron traps in the insulators under the high electrical field. For the gate electron injection case, the gate insulating layer is under high electrical field. The F-P leakage current can be expressed in the following formula [15]:

$$J \sim E \exp(b\sqrt{E}) \quad (1)$$

where  $E$  is the electrical field and  $b$  is the constant at a temperature when the  $I$ - $V$  curve was measured. As shown in the inset of Fig. 6, the calculation of F-P current is in good agreement with the measured  $I$ - $V$  curve. Therefore, the observed  $I$ - $V$  characteristic in  $\text{Mg}_{0.55}\text{Zn}_{0.45}\text{O}$  MIS device shown in Fig. 6 follows high electrical field F-P conduction mechanism. It is worth noting that F-P conduction mechanism dominates over F-N tunneling current, a process whereby electrons tunnel through a barrier between the insulator and semiconductor in the presence of a high electric field, and the Schottky emission which is due to the lowering of potential barrier at the metal-semiconductor contact under high electric field. This means that the density of electrons in the trap and the trap energy in  $\text{Mg}_{0.55}\text{Zn}_{0.45}\text{O}$  films is the main cause of leakage.

#### 4. Conclusion

The cross-section image of TEM for the cubic  $\text{Mg}_{0.55}\text{Zn}_{0.45}\text{O}$  films grown on Si(1 0 0) demonstrates clean interfacial boundary. From the XPS analysis of chemical bonding features near the interfaces of cubic  $\text{Mg}_{0.55}\text{Zn}_{0.45}\text{O}/\text{Si}(1\ 0\ 0)$ , silicon–oxygen bonding has not been observed, indicating that the silicon oxide transition layer can be in monolayer scale. This is attributed to the low growth temperature of  $\text{Mg}_{0.55}\text{Zn}_{0.45}\text{O}$  on Si(1 0 0). The valence band offset of 2.30 eV between cubic  $\text{Mg}_{0.55}\text{Zn}_{0.45}\text{O}$  and Si(1 0 0) is determined by analyzing the valence band spectra of thin  $\text{Mg}_{0.55}\text{Zn}_{0.45}\text{O}/\text{Si}(1\ 0\ 0)$  heterostructure. Using the cubic  $\text{Mg}_{0.55}\text{Zn}_{0.45}\text{O}$  thin films as insulator, MIS structures have been fabricated. Leakage current density as low as  $10^{-7}$  A/cm<sup>2</sup> is obtained at an electrical field of 600 kV/cm. The observed  $I$ - $V$  characteristic in the  $\text{Mg}_{0.55}\text{Zn}_{0.45}\text{O}$  MIS device follows high electrical field F-P conduction mechanism

which indicates that the density of electrons in the trap and the trap energy in the  $\text{Mg}_{0.55}\text{Zn}_{0.45}\text{O}$  film is the main cause of leakage.

#### Acknowledgements

This work was supported by the National Natural Science Foundation of China (No. 10174064) and the Special Funding of Shanghai Nano-Promotion Center (0352NM092).

#### References

- [1] J. Narayan, A.K. Sharma, A. Kvit, C. Jin, J.F. Muth, O.W. Holland, *Solid State Commun.* 121 (2001) 9.
- [2] D.J. Qiu, H.Z. Wu, N.B. Chen, T.N. Xu, *Chin. Phys. Lett.* 20 (2003) 582.
- [3] J. Liang, H.Z. Wu, Y.F. Lao, D.J. Qiu, N.B. Chen, T.N. Xu, *Chin. Phys. Lett.* 21 (2004) 1135.
- [4] N.B. Chen, H.Z. Wu, D.J. Qiu, J. Chen, W.Z. Shen, *J. Phys. Condens. Matter* 16 (2004) 2973.
- [5] N.B. Chen, H.Z. Wu, T.N. Xu, *J. Appl. Phys.* 97 (2005), 023515-1.
- [6] Y. Kwon, Y. Li, Y.W. Heo, M. Jones, P.H. Holloway, D.P. Norton, Z.V. Park, S. Li, *Appl. Phys. Lett.* 84 (2004) 2685.
- [7] S. Masuda, K. Kitamura, Y. Okumura, S. Miyatake, H. Tabata, T. Kawai, *J. Appl. Phys.* 93 (2003) 1624.
- [8] G.D. Wilk, R.M. Wallace, J.M. Anthony, *J. Appl. Phys.* 89 (2001) 5243.
- [9] J. Roberson, *J. Vac. Sci. Technol. B* 18 (2000) 1785.
- [10] J.H. Oh, H.W. Yeom, Y. Hagimoto, K. Ono, M. Oshima, N. Hirashita, M. Nywa, A. Toriumi, A. Kakizaki, *Phys. Rev. B* 63 (2001) 205310.
- [11] S. Miyazaki, *Appl. Surf. Sci.* 190 (2002) 66.
- [12] D.G. Schlom, J.H. Haeni, J. Lettieri, L.F. Edge, Y. Jia, M. Biegalski, V. Vaithyanathan, S.-G. Lim, S. Trolrier-McKinstry, T.N. Jackson, Y. Yang, S. Stemmer, O. Trithaveesak, J. Schubert, S.A. Chambers, H. Li, Y. Wei, K. Eisenbeiser, J.L. Freeouf, C. Hinkle, G. Lucovsky, R. Uecker, P. Reiche, *Si-Compatible Alternative Gate Dielectrics with High  $k$  and High Bandgap*, in: *The 10th International Workshop on Oxide Electronics in Augsburg, Germany*, 2003.
- [13] K.J. Hubbard, D.G. Schlom, *Structure and Properties of Interfaces in Ceramics*, in: *Materials Research Society Symposium—Proceedings*, vol. 357, 1995, p. 331.
- [14] J. Liang, H.Z. Wu, N.B. Chen, T.N. Xu, *Semicond. Sci. Technol.* 20 (2005) 15.
- [15] J. Frenkel, *Phys. Rev.* 54 (1938) 647.